COUPLING THE MARS DUST AND WATER CYCLES: INVESTIGATING THE ROLE OF CLOUDS IN CONTROLLING THE VERTICAL DISTRIBUTION OF DUST DURING N. H. SUMMER.

M. A. Kahre, *NASA Ames Research Center, Moffett Field, CA, USA (melinda.a.kahre@nasa.gov)*, **R. M. Haberle, J.L. Hollingsworth**, *NASA Ames Research Center, Moffett Field, CA, USA*, **R.J. Wilson**, *Geophysical Fluid Dynamics Laboratory, Princeton, NJ, USA.*

Introduction: The dust cycle is critically important for the current climate of Mars. The radiative effects of dust impact the thermal and dynamical state of the atmosphere (Gierasch and Goody, 1968; Haberle et al., 1982; Zurek et al., 1992). Although dust is present in the Martian atmosphere throughout the year, the level of dustiness varies with season. The atmosphere is generally the dustiest during northern fall and winter and the least dusty during northern spring and summer (Smith, 2004). Dust particles are lifted into the atmosphere by dust storms that range in size from meters to thousands of kilometers across (Cantor et al., 2001). During some years, regional storms combine to produce hemispheric or planet encircling dust clouds that obscure the surface and raise atmospheric temperatures by as much as 40 K (Smith et al., 2002). Key recent observations of the vertical distribution of dust indicate that elevated layers of dust exist in the tropics and sub-tropics throughout much of the year (Heavens et al., 2011). These observations have brought particular focus on the processes that control the vertical distribution of dust in the Martian atmosphere. The goal of this work is to further our understanding of how clouds in particular control the vertical distribution of dust, particularly during N. H. spring and summer.

The past few years have seen an increase in the recognition of the importance of water ice clouds on the state of Mars' current climate. The main surface source of atmospheric water is the north residual cap. Broadly, there are two categories of clouds: the aphelion cloud belt and the polar hood clouds. The aphelion cloud belt is composed of optically thin clouds that form above 10-15 km at low latitudes during northern spring and summer (L_s~50°-135°; Clancy et al., 1996). Polar hood clouds form near the edge of the advancing and receding polar cap in both hemispheres during local fall and winter. These clouds are optically thick and may or may not extend down to the surface (Clancy et al., 1996; Benson et al., 2010; Benson et al., 2011).

Cloud formation is the key process for the coupling between the dust and water cycles (Figure 1). Dust particles likely provide the seed nuclei for heterogeneous nucleation of water ice clouds (Montmessin et al., 2002; Maattanen et al., 2007). As ice coats atmospheric dust grains, the newly formed cloud particles exhibit different physical and radiative characteristics. As the mass ratio of ice-to-dust increases, the particle's scattering properties become those of ice instead of dust. The mass and size (and therefore bulk density) of the cloud particles depend on the fraction of ice versus dust. Because the gravitational fall velocity of particles depends on these quantities, cloud formation will either increase or decrease the suspension lifetime of atmospheric dust. The coupling between the dust and water cycles most likely affects the atmospheric distributions of dust, water vapor and water ice and thus atmospheric heating and cooling and the resulting circulation and dynamics. We are interested in how these couplings affect the dust cycle itself.

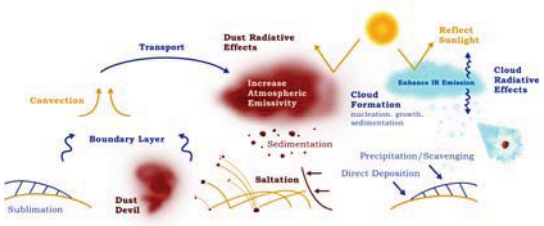

Figure 1: Key processes of Mars' dust and water cycles.

The NASA Ames GCM: The NASA Ames GCM is a 3D finite-difference model of the Martian atmosphere that has been used extensively for investigations of Mars' current and past climate (Haberle et al., 1999; Kahre et al., 2006; Kahre and Haberle, 2010; Hollingsworth and Kahre, 2010). The model runs on a latitude/longitude horizontal grid and a normalized sigma-coordinate vertical grid. For this study, the nominal horizontal resolution is 5° by 6°. Surface properties include MOLA topography and albedo and thermal inertia maps derived from Viking and MGS/TES observations. This version of the model includes a 2-stream radiative transfer scheme that accounts for gaseous absorption and scattering aerosols and a tracer transport scheme based on the Van Leer formulation.

Routines have been incorporated into the GCM to account for the physics of the lifting, transport and sedimentation of radiatively active dust. Two parameterizations for dust lifting, the wind stress and dust devil schemes, are used simultaneously. The wind stress lifting scheme lifts dust when the

momentum imparted to the surface (characterized as the surface wind stress, τ) exceeds a critical value, assumed here to be τ=22.5 mN m^{-2}. The dust devil lifting scheme is based on the thermodynamic theory of dust devils developed by Renno (1998). In this scheme, the lifted dust flux depends on the magnitude of the sensible heat exchange between the surface and atmosphere and the depth of the planetary boundary layer. The lifted dust mass is partitioned into a lognormal distribution with an effective radius of 2.5 μm and an effective variance of 0.5. Airborne dust interacts with solar and infrared radiation, provides seed nuclei for water ice clouds, and undergoes gravitational sedimentation as free dust and as cores of water ice cloud particles. Both dust lifting scheme are tuned with multiplicative "efficiency" factors to produce reasonable dust loadings throughout the Martian year (see, for example, Kahre et al., 2006 for a discussion about tuning).

The simulated water cycle includes sublimation from the north residual cap and the microphysical processes of nucleation, growth, and settling of water ice clouds (Montmessin et al., 2002, 2004). The particle size distribution of cloud particles is represented in the model using a "moment" method, whereby it is assumed that the distribution is lognormal and therefore fully described by a spatially and temporally varying mass and number, and a fixed (constant in time and space) effective variance. This allows for the evolution of cloud and dust particle sizes as the result of microphysical processes in a computationally efficient manner. Water ice clouds can either be radiatively active or inert.

Two simulations are presented: the first includes an interactive dust cycle that is fully coupled to the water cycles through cloud formation; the second includes an interactive dust cycle that does not include cloud formation. In both simulations, the dust lifting schemes are tuned identically (i.e., they have the same efficiency factors), which allows for the most straightforward comparison of the results.

Results: Although both simulations are multi-annual, only results from the first half of one simulated year is shown. Focus is given to the first half of the Martian year in order to quantify the role that clouds in the aphelion cloud belt play in controlling the vertical distribution of dust.

Seasonal Patterns of Dust and Water Ice Clouds: In both simulations, the dust devil lifting scheme is responsible for providing the majority of the atmospheric dust during the first half of the year (L_s 0°-180°). This result is consistent with several previous investigations (Newman et al., 2002; Basu et al., 2004; Kahre et al., 2006). Column 9-μm dust opacities range from zero to a few tenths, which is in general agreement with MGS/TES-observed dust opacities during these seasons (Figure 2). Increased opacities occur along the retreating edge of the seasonal north CO_2 ice cap as the result of increased wind stress lifting during early N.H. spring, particularly in the simulation that includes cloud formation. Radiatively active polar hood clouds in the north increase the baroclinic eddy activity along the growing and receding north CO_2 cap, which leads to increased dust lifting (Hollingsworth et al., 2011; Kahre et al., 2011; Wilson et al., 2011).

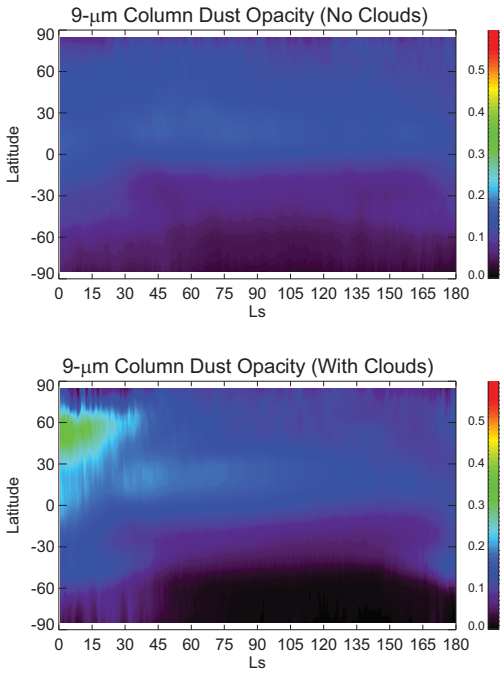

Figure 2: Zonal mean column 9-μm dust opacities during northern spring and summer (Ls=0°-180°) for the simulation without clouds (top) and the simulation with clouds (bottom).

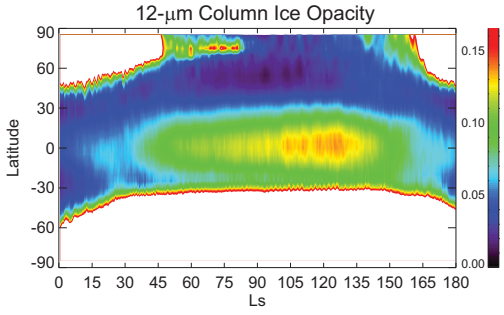

Figure 3: Zonal mean column 12-μm water iceopacities during northern spring and summer (L_s=0°-180°) for the simulation with clouds.

In the simulation with cloud formation, the aphelion cloud belt forms just after the northern vernal equinox, dissipates just before the northern autumnal equinox, and spans from approximately 30

S to 30 N. Column 12-μm ice opacities reach approximately 0.2 slightly to the north of the equator (Figure 3). The spatial extent, seasonality, and column opacity of the simulated aphelion cloud belt is generally consistent with MGS/TES observations (Smith, 2004). Although retrievals of column ice opacities over the seasonal CO_2 ice caps is difficult, comparing the opacities of the edges of the simulated polar hoods to available TES and MCS data suggests that the model is over-predicting the thickness of the polar hoods.

Column-Integrated Dust and Water Ice Cloud Opacities at L_s~120°: Predicted daily mean local column dust IR opacities at L_s~120° range from zero to ~0.5 in the simulations with and without cloud formation (Figure 4). In both simulations, column dust opacities maximize in the Northern Hemisphere over the low thermal inertia continents of Tharsis, Arabia, and Elysium. Simulated dust devil lifting is particularly active in these regions, in part due to the large temperature difference between the surface and the near-surface atmosphere (and thus the sensible heat flux). The most notable differences between the two simulations occur in the Southern Hemisphere. The atmosphere over the south CO_2 seasonal ice cap is clearer of dust in the simulation with cloud formation than in the simulation without, which is directly attributable to the thick polar clouds that form in the former case that effectively scavenge dust from the atmosphere (Figure 5).

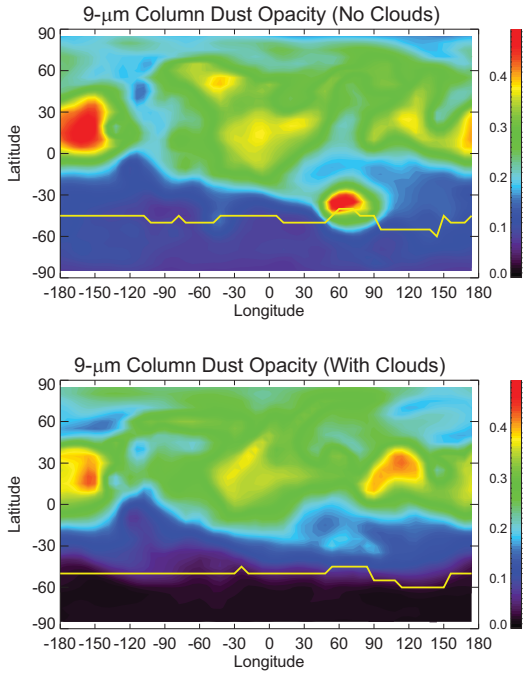

Figure 4: 10-sol mean column 9-μm dust opacities L_s=120° for the simulation without clouds (top) and the simulation with clouds (bottom). The solid yellow line denotes the edge of the seasonal CO_2 ice cap.

Predicted daily mean local column water ice IR opacities at L_s~120° range from zero to >2.0 in the simulation with cloud formation (Figure 5). Optically thick clouds form near the surface over the south seasonal CO_2 ice cap. In general agreement with observations and previous modeling studies, the aphelion cloud belt is zonally asymmetric, with maxima predicted over the high topographic relief regions of Tharsis, Syrtis and Elysium (REFS).

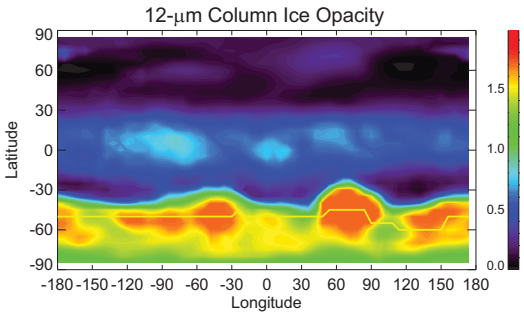

Figure 5: 10-sol mean column 9-μm dust opacities L_s=120° for the simulation without clouds (top) and the simulation with clouds (bottom). The solid yellow line denotes the edge of the seasonal CO_2 ice cap.

Vertical Distribution of Dust and Water Ice Clouds at 15 N at L_s~120°: We focus our analysis at 15 N latitude during the afternoon (i.e., 12-3 pm local time) in order to understand how water ice clouds and their radiative effects in the aphelion cloud belt affect the vertical distribution of dust at low latitudes during N. H. summer.

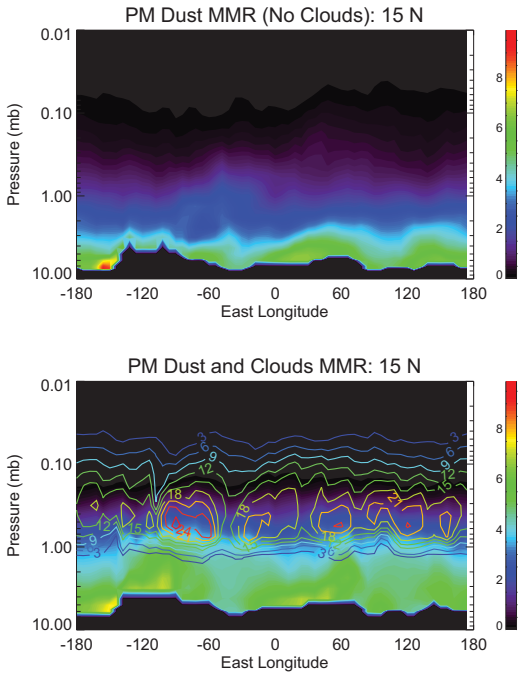

Figure 6: 10-sol mean dust (shaded) and cloud mixing ratios (contoured) at L_s=120° for the simulation without clouds (top) and the simulation with clouds (bottom).

The predicted water ice clouds reside in the afternoon between 1 and 0.1 mbar, with maximum mass mixing ratios occurring at approximately the 0.5 mbar pressure level (Figure 6, bottom panel). These simulated clouds are lower in the atmosphere than MRO/MCS observations suggest at this season (Heavens et al., 2010). While we do not yet understand this discrepancy, it is likely related to the model-predicted thermal structure. This will be a focus of further study in the near future.

There are distinct differences in the predicted vertical distribution of dust between the two simulations (Figure 6). In the simulation with radiatively active cloud formation, the dust is more deeply mixed and falls off with altitude more rapidly than in the simulation without clouds. Preliminary results suggest that dust is more deeply mixed in the cloud case due to the radiative effects of clouds enhancing the strength of the mean overturning circulation (as discussed in Wilson et al., 2007; Madeleine et al., 2012). The more rapid decrease in dust concentration with altitude in the cloud case is likely the combination of two effects: clouds "capping" the dust by scavenging processes and due to increased fall velocities of particles of equal size with increasing altitude (e.g., see Rodin et al. 1999).

Discussion and Conclusions: These results suggest that there are several feedbacks involved in determining the vertical distribution of aerosols in the Martian atmosphere. These feedbacks could involve interactions between the sizes of dust and water ice particle (and their respective fall velocities), dynamical responses to aerosol radiative effects, and possibly dust lifting processes. Although more work needs to be done to fully isolate these feedbacks, it is plausible that the key feedback centers on the interaction between the clouds and the strength and extent of the Hadley circulation. In this scenario, clouds that form in the upper branch of the Hadley cell warm the local atmosphere and intensify the circulation. The circulation then deepens, drawing more water and dust into the upper branch, which mixes the dust more deeply and allows the cloud particles to grow larger and interact more efficiently with the upward IR. The bigger cloud particles and the more deeply mixed dust further intensify the circulation until the cloud particles get big enough to fall faster, which limits further expansion and efficiently "caps" the dust at the level of the clouds.

References:

:w

Basu, S. and M.I. Richardson (2004), Simulation of the Martian dust cycle with the GFDL Mars GCM. *JGR* **109**(46), 11006.

Cantor, B.A., P.B. James, M. Caplinger, and M.J. Wolff (2001), Martian dust storms: 1999 Mars Orbiter Camera observations. *JGR*, **106**, 23653-23687.

Clancy, R.T., A.W. Grossman, M.J. Wolff, P.B. James, D.J. Rdy, Y.N. Billawala, B.J. Sandor, S.W. Lee, and D.O. Muhleman, 1996: Water vapor saturation at low latitudes around aphelion: A key to Mars climate? *Icarus*, **122**, 36-62.

Gierasch, P. J., and R. M. Goody, 1968: A study of the thermal and dynamical structure of the Martian lower atmosphere, *Planet. Space Sci.,* **16**, 615

Haberle, R.M., C.B. Leovy, and J.B. Pollack, 1982: Some Effects of Global Dust Storms on the Atmospheric Circulation of Mars, *Icarus*, ***50*** (2-3), 322-367

Haberle, R. M., *et al*., 1999: General circulation model simulations of the Mars Pathfinder atmospheric structure investigation/meteorology data, *J. Geophys. Res*., **104**, 8957.

Heavens et al., (2010) Water ice clouds over the Martian tropics during northern summer, Geophys. Res. Lett., 37 (18), doi: 10.1029/2010GL044610.

Heavens et al., (2011) The vertical distribution of dust in the Martian atmosphere during northern spring and summer: Observations by the Mars Climate Sounder and analysis of zonal average vertical dust profiles, JGR, 116.

Hollingsworth, J.L., and M.A. Kahre, 2010: Extratropical cyclones, frontal waves and Mars dust: Modeling and considerations. *Geophys. Res. Lett*., **37,** L22202, doi:10.1029/2010GL044262.

Hollingsworth, J.L., M.A. Kahre, R.M. Haberle, and F. Montmessin (2011), Radiatively-active aerosols within Mars' atmosphere: Implications on the weather and climate as simulated by the NASA ARC Mars GCM. *Fourth International Workshop on the Mars Atmosphere: Modeling and Observations,* Paris, France, 8-11 February.

Kahre, M.A., J.R. Murphy, and R.M. Haberle (2006), Modeling the Martian dust cycle and surface dust reservoirs with the NASA Ames General Circulation Model. *JGR*, **111**(E6).

Kahre, M.A., Hollingsworth, J.L., Haberle, R.M., Montmessin, F., (2011): Coupling Mars' Dust and Water Cycles: Effects on Dust Lifting Vigor, Spatial Extent and Seasonality. *Fourth International Workshop on the Mars Atmosphere: Modelling*

and Observations, Paris, France, 8-11 February.

Maattanen, A. Vehkamaki, H. Lauri, A., Napari, I. and Kulmala, M., 2007: Two-component heterogeneous nucleation kinetics and an application to Mars, *Journal of Chemical Physics*, **127**(13), pp. 134710.

Madeleine, J.-B., F. Forget, E. Millour, T. Navarro, and A. Spiga (2012), The influence of radiatively active water ice clouds on the Martian climate, *Geophys. Res. Lett., 39,* L23202, doi10.1092/2012GL053564.

Montmessin, F., P. Rannou, and M. Cabane (2002), New insights into Martian dust distribution and water-ice cloud microphysics. *JGR*, **107**, 5037.

Montmessin, F., F. Forget, P. Rannou, M. Cabane, and R. M. Haberle (2004), Origin and role of water ice clouds in the Martian water cycle as inferred from a general circulation model. *JGR*, **109**, 10004.

Newman, C.E., S.R. Lewis, P.L. Read, and F. Forget (2002), Modeling the Martian dust cycle-2. Multiannual radiatively active dust transport simulations. *JGR*, **107**, 5124.

Renno, N.O., M.L Burkett, M.P. Larkin (1998), A simple thermodynamical theory for dust devils, J. of Atm. Sci., 55 (21).

Rodin, A.V., R.T. Clancy, and R.J. Wilson (1999), Dynamical properties on Mars water ice clouds and their interactions with atmospheric dust and radiation. *Adv. Space. Res*., 23, 1577-1585.

Smith, M.D., Conrath, B.J., Pearl, J.C., Christensen, P.R., 2002. NOTE: Thermal Emission Spectrometer Observations of Martian Planet-Encircling Dust Storm 2001A. *Icarus*, **157** (1) 259-263

Smith, M.D. (2004), Interannual variability in TES atmospheric observations of Mars dust 1999-2003 *Icarus*, **167**(1), 148-165.

Wilson, R.J., G. Neumann, and M.D. Smith (2007), The diurnal variation and radiative influence of martian water ice clouds, *Geophys. Res. Lett*., 34, L02710, doi:10.1029/2006GL027976.

Wilson, R.J. (2011), Dust cycle modeling with the GFDL Mars general circulation model, *Fourth International Workshop on the Mars atmosphere: Modeling and Observations*, Paris, France, 8-11 February.

Zurek, R.W., J.R. Barnes, R.M. Haberle, J.B. Pollack, J.E. Tillman, and C.B. Leovy, 1992: Dynamics of the atmosphere of Mars. *Mars*, H.H. Kieffer, B.M. Jakosky, C.W. Snyder, and M.S. Matthews, Eds., University of Arizona Press, 835–933